Title
Visualization of Volumetric Structures from MR Images of the Brain

Authors
Parvin, B.
Johnston, W.
Robertson, D.

Publication Date
1994-03-01

LBL-35325
UC-405

Lawrence Berkeley Laboratory
UNIVERSITY OF CALIFORNIA

Information and Computing Sciences Division

Presented at the AAAI Conference on Application of Computer Vision to Medical Imaging, Palo Alto, CA, March 21–23, 1994, and to be published in the Proceedings

Visualization of Volumetric Structures from MR Images of the Brain

B. Parvin, W. Johnston, and D. Robertson

March 1994

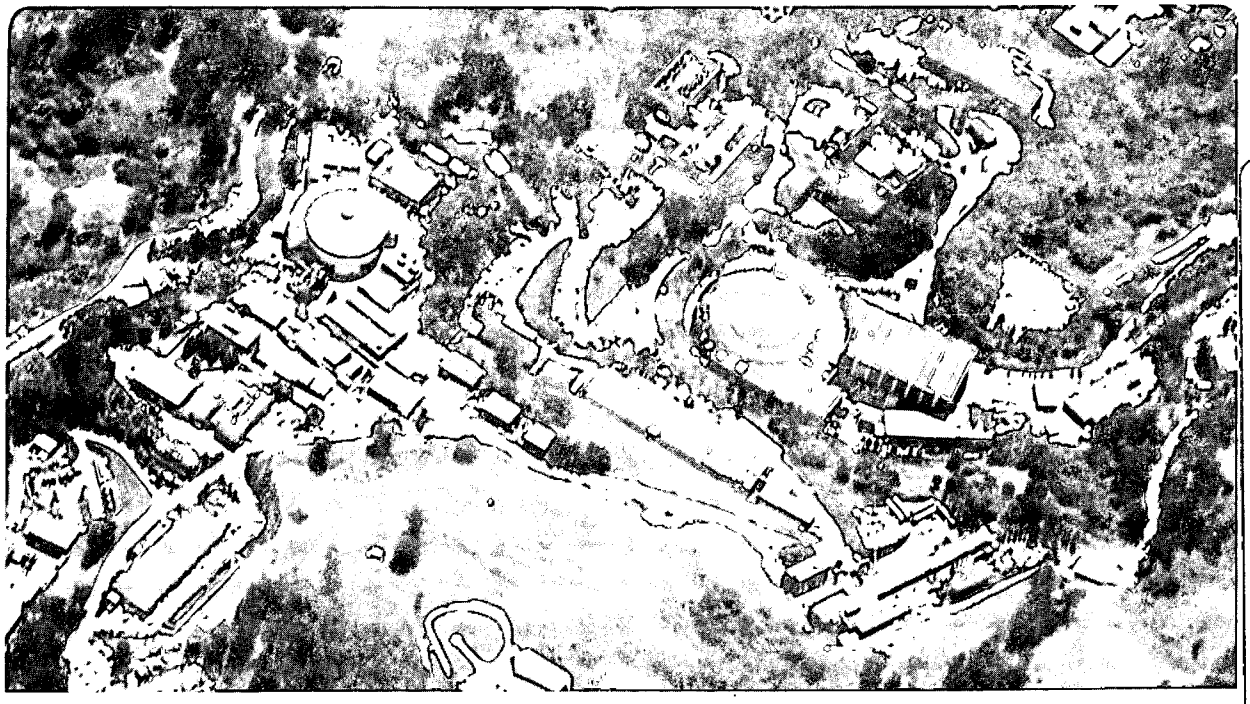

Prepared for the U.S. Department of Energy under Contract Number DE-AC03-76SF00098

DISCLAIMER

LBL-35325

Visualization of Volumetric Structures from MR Images of the Brain

B. Parvin, W. Johnston and D. Robertson
Information and Computing Sciences Division
Lawrence Berkeley Laboratory
University of California
Berkeley, CA 94720

This work was supported by the U.S. Dept. of Energy, Office of Scientific Computing, under Contract DE-AC03-76SF00098

Visualization of Volumetric Structures from MR Images of the Brain

B. Parvin, W. Johnston and D. Robertson
Information and Computing Sciences Division
Lawrence Berkeley Laboratory
University of California
Berkeley, CA 94720

Abstract

Pinta is a system for segmentation and visualization of anatomical structures obtained from serial sections reconstructed from magnetic resonance imaging. The system approaches the segmentation problem by assigning each volumetric region to an anatomical structure. This is accomplished by satisfying constraints at the pixel level, slice level, and volumetric level. Each slice is represented by an attributed graph, where nodes correspond to regions and links correspond to the relations between regions. These regions are obtained by grouping pixels based on similarity and proximity. The slice level attributed graphs are then coerced to form a volumetric attributed graph, where volumetric consistency can be verified. The main novelty of our approach is in the use of the volumetric graph to ensure consistency from symbolic representations obtained from individual slices. In this fashion, the system allows errors to be made at the slice level, yet removes them when the volumetric consistency cannot be verified. Once the segmentation is complete, the 3D surfaces of the brain can be constructed and visualized.

1 Introduction

Pinta is a system designed for automatic segmentation, visualization, and description of the human brain from magnetic resonance images. The ultimate objective of this system is to provide a research vehicle for gaining new insights into structural changes in the brain over time and across individuals. In this paper, we focus on the segmentation and visualization aspects of our system, since the volumetric description is the subject of our continued research. In practice, MR images can be tuned to accentuate certain anatomical structures. For example, by applying a specific pulse sequence, the boundary separation between *cerebrospinal fluid* (CSF), *gray*, and *white* matter can be maximized. From this perspective, the segmentation procedure should label each pixel in the data volume accordingly. However, there are a number of ambiguities that can complicate the labeling process. These ambiguities can arise from purely local processing and the absence of any high level feedback. The sources for the ambiguities include corruption of data by noise, performance limitation of algorithms for extracting local features, and existence of nonessential features that impede the labeling task. Our approach to the segmentation process is to exploit the knowledge of the anatomical structures coupled with the image characteristics and arrive at a correct labeling. In this sense, the segmentation is model driven, where the model is expressed in terms of anatomical constraints and certain knowledge about the image formation. From an anatomic standpoint, the cerebral cortex is a single sheet of convoluted structure [2]. And from the image formation perspective, certain intensity distributions reflect the presence of CSF and white and gray matter. Hence, we have organized various constraints at different levels of the computational hierarchy so that stable labeling can be realized.

A computational framework will have a different performance depending upon the coarseness of low level representations. For example, low level representations, such as edgel or local texture, are easy to compute. However, these low level representations complicate the reasoning task. On the other hand, high level representations, such as regions or symmetries, simplify the reasoning task, but the algorithms to compute them are usually expensive. The important issue is to maintain the proper balance so that the system can generate a modest amount of hypotheses - not all of them correct- which can be verified or rejected at a higher level. This is an important feature of our system that is achieved through proper region segmentation at the slice level followed by testing for anatomical consistency at the volumetric level.

The region based segmentation relies on clustering and relaxation, where the clustering is performed in the *feature* space. The clustering step refines the center of the mass for each class, and the relaxation step ensures local consistency. The system applies the necessary verification step to ensure that the result of clustering is anatomically correct (based on the knowledge of image intensity distribution in the cortex). Each slice of the image is represented with an attributed graph, where nodes correspond to regions and links correspond to the relations between regions. These attributed graphs are then coerced together to form a volumetric attributed graph, where 3D consistency can be verified. In this manner, the system tolerates erroneous labeling at the slice level, and then removes them at higher levels of processing.

In the next section, we review the previous work and compare their respective features. In section 3, we discuss the details of our approach and provide results on real data.

2 Past work

Most of the previous research on this topic can be partitioned into four categories. These include 1) interactive systems, 2) classification based techniques, 3) knowledge based systems and 4) contour based techniques.

The classification based techniques [9] require training data and lack the necessary structural analysis. Our ex-

*Research was supported by the U.S. Dept. of Energy, Office of Scientific Computing, under Contract DE-AC03-76SF00098

perience indicates that purely tissue based classification is not sufficient for a robust system. This will become clear in the examples given in the next section.

The knowledge based systems include the ruled-based system of Raya [11] and the blackboard architecture of Chen [3]. Raya's system makes a strong use of connectivity information across two channels of information, namely proton density (PD) and T2-weighted MR images. At each pixel location, a vector is derived to represent the local feature activities. The inference engine then uses these feature vectors to partition the data volume across the anatomical boundaries. Chen's system uses CT data, in addition to PD and T2-weighted, to generate the necessary hypotheses. This system generates a large number of initial hypotheses that are grouped together based on a multivariate belief function. All of the hypotheses are generated from multichannel 2D slices, and 3D information is not utilized. The main disadvantage of these techniques is that their low level processing is very weak; thus, the knowledge based system has to deal with a large number of hypotheses and maintain a large set of (non-obvious) rules to deal with the inherent ambiguities. Furthermore, the ruled-based techniques tend to be slow when they have to process large amounts of data. There is a great degree of complexity in using multimodal data, and it is not clear that images from two or three modalities are needed to infer anatomical structures.

The contour based techniques include the work of Bomans [1] and Wu [13]. Bomans proposed extracting essential anatomic structures with a 3D extension of the Marr-Hildreth filter. The zero crossing filter was applied at a single scale, which was selected empirically. The main advantage of the techniques is that volumetric closure is guaranteed through continuous zero crossings. They then corrected the localization error of the zero-crossing filter through a sequence of morphological operators. The same result could have been obtained with scale space filtering or edge focusing. Finally, the volumes of interest were *manually* labeled, and the surfaces were rendered for visualization. The main disadvantage of this technique, or any other edge based approach, is that the boundary between gray and white matter is often indistinct. As a result, the correct segmentation is not ensured. Wu and Leahy [13] presented an elegant graph theoretic approach, where contour closure from local edges is enforced by optimizing the maximum flow in an image represented by a graph. Yet, their approach ignores the 3D information of the data set and suffers from an excessive computational burden. Nevertheless, the work is significant from the standpoint of graph theory and a class of problems in computer vision.

3 Description of the method

In our view, segmentation is the final objective in any interpretation process, and should not be confined to some low level processes. In this context, segmentation of MRI should partition and match 3D regions to anatomical structures. There are two major components to our system. The first one operates on slice level information and generates an attributed graph. In this component, local consistency at the pixel level, together with slice level region consistency, is enforced to reduce the number of potential hypotheses. The second component operates on the volumetric attributed graph and ensures 3D consistency. The architecture of this system is shown in figure 1, where the feedback loop ensures correct segmentation at each level of the hierarchy.

In this system, we build a symbolic description from each slice, and let the volumetric step extract relevant attributes from these symbolic descriptions. The segmentation technique is model driven, where the model is represented in terms of anatomical constraints. For example, we know that ventricles are present at a certain distance from the top of the skull. These modeling cues are used to initiate the segmentation process from a particular slice called the *seed frame*. In the seed frame, the ventricles are detected through their intensity distribution and shape symmetries and then tracked in adjacent slices.

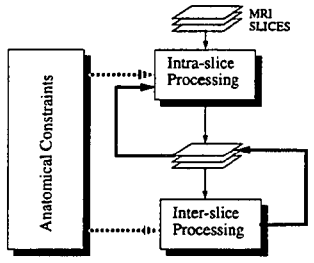

Figure 1: System Architecture

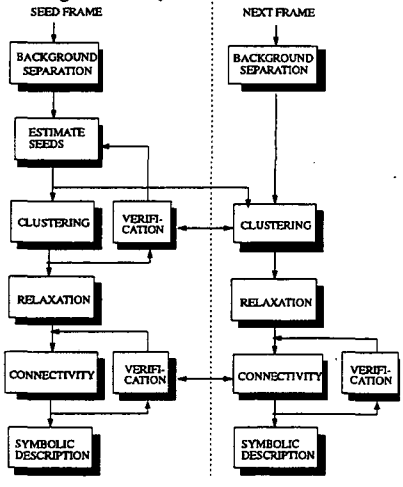

Figure 2: Intra-slice Processing

3.1 Intra-slice processes

There are two parts in this subsystem. The first one groups neighboring pixels with similar properties (low level processing) and builds an initial symbolic description. The second part searches for a particular structure and corrects for erroneous labeling.

The initial symbolic description is a region based segmentation. We use the intensity values of the pixels to group nearby pixels into homogeneous patches. The justification for using the intensity value is based on *i)* a moderate amount of shading, and *ii)* the small number of distinguishable regions that are usually significant. A careful analysis of MRI data, obtained in the T1-relaxation mode, reveals that four-class region segmentation is sufficient for extracting the important patches from brain scans. The architecture for the intra-slice component of the system is shown in figure 2, and the details of each module are summarized below.

The first step of our computational process is to create a mask that excludes the background area. In addition, the outer boundary of the skull is also extracted and a proximity map is constructed that encodes the distance of each pixel from the skull boundary. The four classes in the region segmentation correspond to: i) *cerebrospinal fluid* (CSF) or bone, which are the darkest region in MRI data; ii) *gray matter* corresponding to neuronal cell bodies; iii)

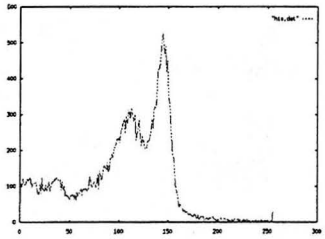

Figure 3: Global histogram

white matter corresponding to nerve fibers; and iv) *others* corresponding to high contrast objects that could include tumors.

The key to region segmentation is in estimating the average intensity of each region. This is done by analyzing the histogram, followed by clustering. In a *seed frame*, the histogram, as shown in figure 3 is approximated by a quadratic B-spline and the peaks are determined analytically. Generally, the peaks corresponding to gray and white matter are distinctly visible in the histogram. However, the peak corresponding to the CSF can be buried in the background if the seed frame is not selected properly. In our system, we choose the seed frame such that the ventricles occupy a modest area of the image; thus, their intensity distribution is accentuated. The peaks are then used as *feature seeds* for initiating the clustering.

The clustering technique is a variation of K-means clustering procedure, which is a well known technique. Anatomically, we know that gray and white matter share an edge. Therefore, the cluster centers are verified by searching the gray-level co-occurence matrices. This process of seed estimation and verification is performed only on the seed frame, and the same seeds are then used in every consecutive slice. Clustering is essentially in the feature space and ignores any spatial constraints in the image domain. The next step of the computational process is to use the cluster centers to enforce local consistency in the image space. We use a probabilistic relaxation model to implement this step of the process. This is an iterative scheme, where local properties are propagated and noise is removed by enforcing consistency. The initial labeling, P_i, is based on the proximity of each pixel, i, to one of the four clusters. In the following formulation, vectors are represented by upper case characters. Let

1. k_1, through k_4 denote the labeling of the four classes,
2. $p_i(k_j)$ be the probability of assigning pixel i to class k_j.
3. $q_i(k_j)$ be the compatibility of pixel i with class k_j. The compatibility is a measure of local support for the center pixel. If the local gradient is small, then the compatibility is defined as the local mean probability around the eight nearest neighbors, that is:

$$q_i(k_j) = \frac{1}{8} \sum_{j \in local(i)} p_i(k_j) \qquad (1)$$

Otherwise, the compatibility is defined as the local mean probability along the directional derivative. In this fashion, smoothing is enforced only in the interior of the region. The gradient threshold is computed directly from the distance between the centers of clusters.

The relaxation algorithm can now be defined as a labeling that minimizes the following global criterion.

$$Minimize \;\; C = -\sum_{i=1}^{n} \vec{P}_i \bullet \vec{Q}_i \qquad (2)$$

$$subject \;\; to \;\; constraints \; p_i(k_j) > 0 \; and \; \sum_{j=1}^{4} p_i(k_j) = 1 \qquad (3)$$

The constraint minimization problem can now be solved with the gradient projection method. The solution to the above problem is given by

$$P_i^{n+1} = P_i^n + \alpha \mathcal{P}(\vec{d}) \qquad (4)$$

where α is the step size, $\mathcal{P}$ is the projection operator defined over the space of active constraints and $\vec{d}$ is the feasible direction. At the completion of the above computational process, each pixel is labeled as a member of one of the four different categories. However, we are also interested in extracting regions that are perceptually significant; for example, ventricles that are displayed by large symmetrical black regions along the Z axis. In the cerebral cortex, symmetries are mirrored geometric transformations from the left to the right side of the brain.

In summary, the intra-slice component utilizes intensity features to hypothesize regions. Two examples of slice level processing are shown in figures 4. Note that some of the *membrane* tissues are also labeled as white matter at the slice level labeling; however, these errors will be corrected at the higher level process.

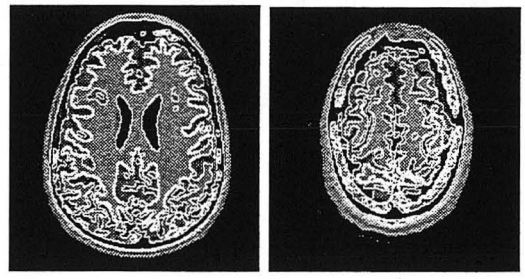

(a) (b)

Figure 4: Slice level grouping

3.2 Inter-slice subsystem

At the completion of the previous stage, the content of each slice is symbolically represented as an attributed graph. The nodes and links in the graph correspond to regions and relationships between regions, respectively. The inter-slice process goes beyond the evidence in a given slice and attempts to resolve ambiguities that can be corrected through volumetric analysis. For example, we have already indicated that the white matter is a singly convoluted structure. This anatomical constraint translates into 3D connectivity among all regions that are labeled as white matter in each slice. Thus, any erroneously labeled region can be removed using a simple binary constraint. Furthermore, gray matter should share a boundary with the white matter. Therefore, any isolated gray matter can be removed from the list of active hypotheses. An example of volumetric consistency, corresponding to examples shown in figure 4, is shown in figure 5. Another example of intra-slice and inter-slice processing is shown in figure 6, where part of the white matter has changed its characteristic due to an apparent stroke.

3.3 Visualization from serial sections

Visualization has been the subject of much research. The simplest way to compute *3D surfaces* is by triangulation

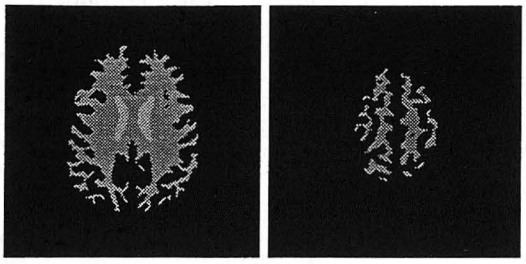

(a) (b)

Figure 5: Volumetric level grouping

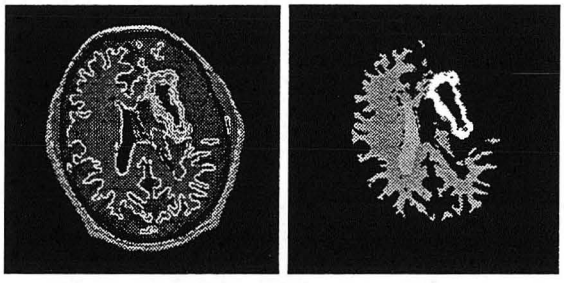

(a) (b)

Figure 6: Slice level and volumetric level grouping for the stroked patient

between adjacent pairs of contours. This is adequate for surfaces that are almost convex. Yet, triangulation becomes ambiguous when the surface topology changes rapidly. An alternative is to find the intersection of a surface with each volume element in the data. An example of this approach is the dividing cubes method [6]. Our system uses dividing cubes, with the modification that the surface is selected using volumetric segmentation information rather than thresholding. Surfaces representing segmented data are shown in Figures 7 and 8. Figure 7 shows a top and a bottom view of the white matter in a 256x256x60 data set of a healthy brain. Figure 8 is obtained from a data set from a patient suffering from a stroke.

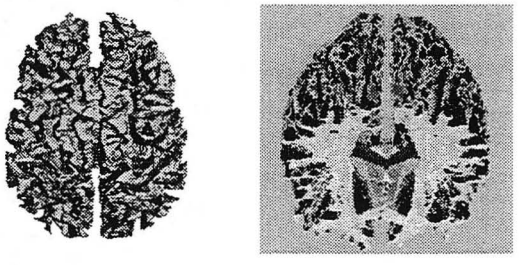

(a) (b)

Figure 7: Surface reconstruction and rendering from two views: (a) white matter; (b) two isosurfaces corresponding to white matter and ventricle.

4 Conclusion

In this paper, we have presented a computational scheme for segmentation of magnetic resonance images. Our computational model decomposes the solution into slice and volumetric level processing. In the intra-slice step, the major assumption is that the each slice can be decomposed into four classes, and in the inter-slice step, the main assumption is that the ambiguities can be resolved with binary constraints. Our current research focuses on the description of these complex superstructures and how they relate to one another.

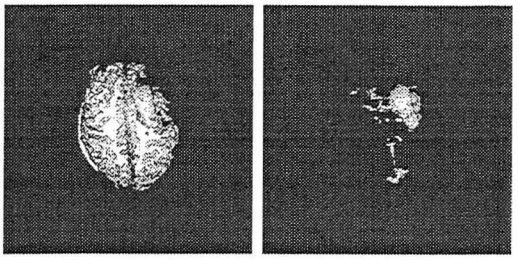

(a) (b)

Figure 8: Surface reconstruction and rendering from two views of the stroked cortex: (a) white matter and stroked area; (b) impact of the stroke.

Acknowledgments: The authors thank Dr. Tom Budinger and Greg Klein of the research medicine group at LBL, and Mr. Scott Buchanan of *BTI* for supplying the data for this research.

References

[1] M. Bomans, et al, "3D Segmentation of MR images of the head for 3D Display," *IEEE Trans. on Medical Imaging*, Vol. 9, 1990, pp.177-183.

[2] M. B. Carpenter, *Core Text of Neuroanatomy*, Third edition, Williams and Wilkins, 1984.

[3] S.Y. Chen, et al, "Spatial Reasoning Based on Multivariate Belief Function," *IEEE Conf. on Computer Vision and Pattern Recognition*, 1992, pp. 624-626.

[4] D. Kennedy, et al, "Anatomic Segmentation and Volumetric Calculations in Nuclear Magnetic Resonance Imaging," *IEEE Trans. on Medical Imaging*, Vol. 8, 1989, pp.1-7.

[5] D. Levin, X. Hu, K. Tan and S. Galhotra, " Surface of the Brain: Three-dimensional MR images created with Volume Rendering," *Radiology*, Vol. 171, 1989, pp. 277-280.

[6] H.E. Cline, W.E. Lorensen, et.al., "Two Algorithms for the three-dimensional reconstruction of tomograms," *J. of Medical Physics*, Vol. 15, No.3, June 1988, pp.320-327.

[7] D. Luenberger, *Introduction to Linear and Nonlinear Programming*, Addison Wesley, 1973.

[8] J. Mazziotta, et al., "Relating Structure to Function in vivo with Tomographic Imaging," *1991 Exploring Brain Functional Anatomy with Positron Tomography, Wiley, Ciba Foundation Symposium 163*, pp.93-112.

[9] K. Oshio and M. Singh, "Neural Network Approach to Segmentation of Magnetic Resonance Head Images," *Int. Journal of Imaging Systems and Technology*, 1992, pp. 130-134.

[10] B. Parvin, W. Johnston and D. Roselli,"Pinta: A System for Visualizing the Anatomical Structures of the Brain from MR Imaging," *IEEE Conf. on Computer Vision and Pattern Recognition*, June 1993, p.615.

[11] S. Raya, "Low-level Segmentation of 3D Magnetic Resonance Brain Images-A Rule-base System," *IEEE Trans. on Medical Imaging*, Vol. 9, 1990, pp.327-337.

[12] D. Robertson, et. al., "Distributed Visualization Using Workstations, Supercomputers, and High Speed Networks," *IEEE Visualization*, 1991, 379-382.

[13] Z. Wu and R. Leahy, "Image Segmentation via Edge Contour Finding: A Graph Theoretic Approach," *IEEE Conf. on Computer Vision and Pattern Recognition*, 1992, pp. 613-619.

LAWRENCE BERKELEY LABORATORY
UNIVERSITY OF CALIFORNIA
TECHNICAL INFORMATION DEPARTMENT
BERKELEY, CALIFORNIA 94720